# Near-future changes in storm surges along the Atlantic Iberian coast

André B. Fortunato[1]; Edmund P. Meredith[2]; Marta Rodrigues[3]; Paula Freire[4]; Hendrik Feldmann[5]

Submitted: January 2, 2018; reviewed: April, 2018; accepted: May 23, 2018; available online: May 29, 2018

This is a post-peer-review, pre-copyedit version of an article published in Natural Hazards. The final authenticated version is available online at: https://doi.org/10.1007/s11069-018-3375-z. Please cite this paper as:

Fortunato, A.B., Meredith, E.P., Rodrigues, M., Freire, P., Feldmann, H. (2019). Near-future changes in storm surges along the Atlantic Iberian coast, *Natural Hazards*, DOI: 10.1007/s11069-018-3375-z

**Abstract**

Decadal predictions bridge the gap between the short-term weather/seasonal forecasts and the long-term climate projections. They target the reproduction of large-scale weather patterns at multi-year time scales by both recognizing the long memory of some components of the climate system, and explicitly including the evolution of green-house gas concentrations as an external forcing. This study illustrates the use of decadal predictions to determine the near-future storminess at regional scales. Specifically, the evolution of extreme storm surges and sea levels along the Atlantic Iberian coast is assessed. Present (1980-2016) and near-future (2021-2024) storm surges are simulated over the north-east Atlantic, forced by atmospheric reanalyses (ERA-Interim) and decadal predictions (MiKlip), respectively. Results are then statistically analyzed to investigate the short-term effects of climate change and climate variability on extreme surges and extreme sea levels. Surges will increase mostly in early winter, while tides are largest in late winter. As a result, the impact of the increase in storminess on the extreme sea levels and coastal flooding will be modest, and the growth in extreme sea levels will be dominated by the contribution of mean sea level rise.

**Keywords**: storm surge, numerical modeling, SCHISM, decadal prediction, Portugal, Spain

[1] Corresponding author. National Laboratory for Civil Engineering, Av. do Brasil 101, 1700-066 Lisbon, Portugal. ORCID: 0000-0003-4667-1945. Email: afortunato@lnec.pt; phone: +351 21 844 3425.

[2] Institut für Meteorologie, Freie Universität Berlin, Carl-Heinrich-Becker Weg 6-10, D-12165, Germany. ORCID: 0000-0001-7555-0005

[3] National Laboratory for Civil Engineering, Av. do Brasil 101, 1700-066 Lisbon, Portugal. ORCID: 0000-0002-9926-1918

[4] National Laboratory for Civil Engineering, Av. do Brasil 101, 1700-066 Lisbon, Portugal. ORCID: 0000-0001-9801-6008

[5] Institute for Meteorology and Climate Research (IMK-TRO), Karlsruhe Institute of Technology (KIT), POB 3640, 76021 Karlsruhe, Germany

## 1. Introduction

Floods of marine origin constitute a major natural hazard, responsible for countless casualties and severe damage every year (Chaumillon et al. 2017). The year 2017, with eight consecutive hurricanes in the western Atlantic in a six-week period, provides abundant examples of the devastation caused by marine submersions in Central and North America. Climate change is aggravating this hazard through an accelerating sea level rise (SLR) (Dangendorf et al. 2017) and increased storminess in some regions (Thompson et al. 2013). Simultaneously, the growth of population density in coastal regions increases the vulnerability to these hazards. There is therefore a growing interest in quantifying the intensity and frequency of extreme events at the coast, and how the associated hazard will evolve in the future.

The present study aims at analyzing how the flood hazard is predicted to evolve in the near future along the Atlantic Iberian coast due to changes in atmospheric and ocean forcings. This area has generally been spared from major marine floods in the past decades. Yet, this absence of catastrophic events can cause a sense of security and a lack of preparedness that may aggravate the consequences of a major storm. For instance, a major storm hit this coast in February 1941, causing dozens of victims and widespread destruction (Muir-Wood 2011; Freitas and Dias 2013; Garnier et al. 2018). If it were to happen today, this storm would cause €5 billion worth of damage (Muir-Wood 2011) and extensive flooding along the margins of the Tagus estuary (Fortunato et al. 2017). Hence, this hazard should be taken seriously.

Recent studies suggest that the future growth of the flooding hazard in this area will be milder than in many other regions of the world. Analyses of tidal gauge records indicate that the past growth of extreme sea levels in the Iberian Atlantic coast is mostly explained by SLR (Marcos and Woodworth 2017). The same authors found that non-tidal residuals in this coast had negligible or even negative trends. Several studies also indicate that wave conditions in the Iberian coast will not be aggravated by climate change (Andrade et al. 2007; Charles et al. 2012; Perez et al. 2015; Camus et al. 2017). Similarly, Vousdoukas et al. (2016) found that storm surge levels in southern Europe will be stable or even decrease in the present century. Recently, Vousdoukas et al. (2017) modeled the increase in extreme sea levels along the European coast during the 21$^{st}$ century. These authors concluded that reductions of extreme surges and waves along the Portuguese coast could actually offset SLR by the end of the 21$^{st}$ century, leading to a reduction in extreme sea levels. However, these authors approximated the wave setup as 20% of the significant wave height. Recent findings indicate that this approximation is an over-prediction (Guérin et al 2018). The conclusions of Vousdoukas et al. (2017) may thus be too optimistic in regions where extreme waves will decrease in the future.

In order to analyze the evolution of extreme storm surges and water levels along the Iberian Atlantic coast in the next decade, we take advantage of a recently developed set of decadal predictions (MiKlip) to reduce the near-future uncertainty found in uninitialized earth system models (ESMs). The MiKlip collaboration (Marotzke et al. 2016) is developing a world-class decadal prediction system. Unlike climate projections, which focus on changes in climatological statistics in response to enhanced greenhouse gas forcing, decadal predictions (e.g. Smith et al. 2007) additionally seek to model near-term (i.e. $\leq$ 10 years) changes in the climate system due to natural internal variability, which can often be much stronger than the local climate change signal (e.g. Bordbar et al. 2017). This is achieved by initializing the ESM with the observed state of the climate system, and the prediction skill is derived from the long-term memory of certain climate system components, e.g. ocean and soil. Hence, decadal predictions do not aim to represent the full range of climatological variability, but rather to predict the range of variability most likely over the coming decade. The first phase of MiKlip (baseline-0) exhibited improved skill over its forerunners, particularly over the North Atlantic (Mueller et al., 2012). The second phase (baseline-1, used herein), in

which an improved initialization was introduced, shows further improved skill, especially in the tropics (Pohlmann et al. 2013). MiKlip additionally has a significant skill in predicting the statistics of extra-tropical cyclones, especially over the Pacific and North Atlantic (of relevance to the Iberia region), and in particular for the most intense cyclones (Kruschke et al. 2014, 2016). To account for the inherent uncertainty in initial conditions, MiKlip produces a ten-member ensemble of predictions for each initialization year. Here, the present is taken as the period 1980-2016, and the future as 2021-2024. The "present" is thus centered on 1998, and the future on 2022. Since the focus is on the near future, the difference between RCPs is negligible and a single scenario (RCP4.5) is thus considered.

This paper is organized in three sections besides this introduction. The methods are described first, including the models and the statistical treatment of the results. Results are presented and discussed next. The major conclusions are summarized in the last section.

## 2. Methods

### 2.1. Drivers of extreme sea levels

Extreme sea levels are caused by the combined effect of several agents: mean sea level, tides, atmospheric pressure, wind and waves. Each of these agents will be affected by climate change.

Global SLR predictions for the end of the 21$^{st}$ century show a large variation, mostly associated with RCP scenarios. However, the uncertainty is much smaller at shorter time scales. For instance, Nauels et al. (2017) estimated global SLR for four alternative scenarios (RCP2.6, RCP4.5, RCP6.0 and RCP8.5). Considering only the period 2000-2023, the four projections are very similar (about 11 cm). Although the regional variation in SLR can be significant, global projections are generally adequate for the Iberian Peninsula. Guerreiro et al. (2015) points out that the upward vertical movement at Cascais is an order of magnitude smaller than SLR. Santamaría-Gómez et al. (2017) computed the vertical land motion at many stations worldwide, and results indicate that, at most Iberian coastal stations, this motion is smaller than 0.5 mm/year (http://www.sonel.org), an order of magnitude smaller than the present SLR trend in the region. Also, the estimated 11 cm rise in sea level between 2000 and 2023 is consistent with the latest estimates of SLR at Cascais (Antunes 2016): 4.1 mm/year, with a slight acceleration. Predictions of future SRL rates in the same area for the period 2007-2024, taken from http://icdc.cen.uni-hamburg.de/1/daten/ocean/ar5-slr.html are similar: 4.0 mm/year (RCP4.5) and 4.2 mm/year (RCP8.5). Hence, the global estimate of 11 cm will be used henceforth.

Pickering et al. (2017) determined the response of tidal amplitudes to SLR. The response is spatially complex and can be significant in some areas. However, the impacts of SLR on the tidal amplitude in the Iberian shelf will be small, possibly due to the narrow continental shelf. For instance, a uniform rise of 2 m in the mean sea level would increase the mean high water level by up to 3 cm. Assuming a linear response, following Idier et al. (2017), the changes in tidal amplitude are an order of magnitude smaller than the driving SLR and will be neglected herein.

Wave-induced setup can increase the sea level at the coast and depends primarily on the significant wave height. For instance, Guérin et al (2018) found wave setups of about 10-15% of the significant wave height for different energetic conditions. In areas of the world where wave energy is increasing due to climate change, an associated growth in wave-induced setup should thus be anticipated. However, several studies indicate that wave conditions in the Iberian coast will not be aggravated by climate change (Andrade et al. 2007; Charles et al. 2012; Perez et al. 2015; Camus et al. 2017). This trend justifies

ignoring the wave setup in this study. Still, this is a limitation of the modeling approach followed herein, and in most similar studies, and future efforts should attempt to take wave setup into account.

Finally, the effect of wind and atmospheric pressure on water levels is determined by running atmospheric and ocean models. Multi-decadal simulations are performed, so that statistical analyses can be performed on the results and extreme conditions can be extrapolated. The modeling procedures and the statistical analyses are described below.

## 2.2. Atmospheric modeling

This study incorporates two sets of atmospheric forcings, representative of the (i) present day (ERA-Interim, Dee et al. 2011) and (ii) near future (MiKlip decadal predictions).

For the decadal predictions, a 10-member ensemble of 4-year predictions (2021-2024) with different initial conditions was taken from the MiKlip system, the Max Planck Institute's ESM with low-resolution stratosphere (MPI-ESM-LR; see Giorgetta et al. 2013). The 10-member ensemble is created via lagged initialization (Pohlmann et al., 2013), i.e. individual members are initialized on consecutive days centered on January 1$^{st}$, 2015. This increased ensemble size, relative to earlier stages of the MiKlip project, has been shown to increase skill for all lead years (Kadow et al., 2016). Increased ensemble size additionally allows the ensemble spread to better represent initial-conditions-related uncertainty (Kadow et al. 2016); additional sources of uncertainty in decadal predictions are discussed in Marotzke et al. (2016). MPI-ESM-LR has a horizontal resolution of T63 (~1.875°/205 km), 47 vertical levels, and a model top at 0.1 hPa. All members were subsequently dynamically downscaled to 0.44° (~50 km) resolution over the EURO-CORDEX domain (Jabob et al. 2014) with the COSMO-CLM model (CCLM; Rockel et al. 2008), version 4.8. CCLM is the non-hydrostatic community model of the German regional climate research community jointly further developed by the CLM-Community. Greenhouse gas concentrations follow RCP4.5 (Van Vuuren et al. 2011). The model setup includes 40 unevenly spaced terrain-following vertical levels (with a higher concentration of levels near the surface), a 250 km relaxation zone at the lateral boundaries, the Tiedtke convection scheme (Tiedtke 1989), and a time step of 240 seconds with a third order Runge-Kutta integration scheme. The 0.44° CCLM simulations, dynamically downscaled from MPI-ESM-LR, are used to force the oceanic models described in Section 2.3.

This study analyses the final years (2021-2024) of the decadal predictions (baseline-1), representing lead years 7-10 of the 10-year predictions. Focusing on the final years of the decadal predictions is expected to better highlight the effects of any externally-forced signals to emerge. While, in general, the memory of the climate system decreases with lead time, the skill scores for storm activity in Europe and the North Atlantic are actually higher for lead years 2-9 than for lead years 2-5 when compared against climatological forecasts (Kruschke et al., 2016). Hence, considering the final years of the decadal predictions should not increase the uncertainty in the predictions.

Although the MiKlip decadal hindcasts have been validated in previous publications (e.g., Kruschke et al. 2014, 2016), an additional validation was performed, focused on the Iberian Peninsula (Fig. 1). Since storm surges in this region are mostly due to low atmospheric pressures, an extreme value analysis was performed for low atmospheric pressure. Extremes were determined for the period 1980-2014 for (a) the ERA-Interim reanalysis, and (b) a 10-member ensemble of continuous historical simulations with the MPI-ESM-LR model downscaled with the CCLM model to 0.44º resolution (i.e. the same model used in the MiKlip prediction system); we are thus comparing the two global models used to force our regional model. All ten members of the ensemble were included individually in the analysis, and only lead years 7 through 10 were retained, to be consistent with the lead years used in the near-future simulations.

Generalized Extreme Value (GEV) distributions were then fitted to the series of annual minima (see section 2.4 for details). Results suggest a small bias in the MPI-ESM-LR model. At the south and west coast stations (Huelva, Lagos, Cascais and Leixões) the differences are smaller than 3 hPa. Considering only the inverse barometer effect, this difference in pressure will lead to a difference of the order of 3 cm in the storm surge (e.g., Chaumillon et al. 2017) and is neglected henceforth. At the stations in the north coast (La Coruna and Bilbao), the discrepancy between the two curves grows with the return period, reaching 8 hPa at Bilbao for a return period of 100 years. This growth can be due to model errors, but also to the uncertainty associated to the extreme value analysis method (see Wahl et al., 2017 for an analysis of this uncertainty).

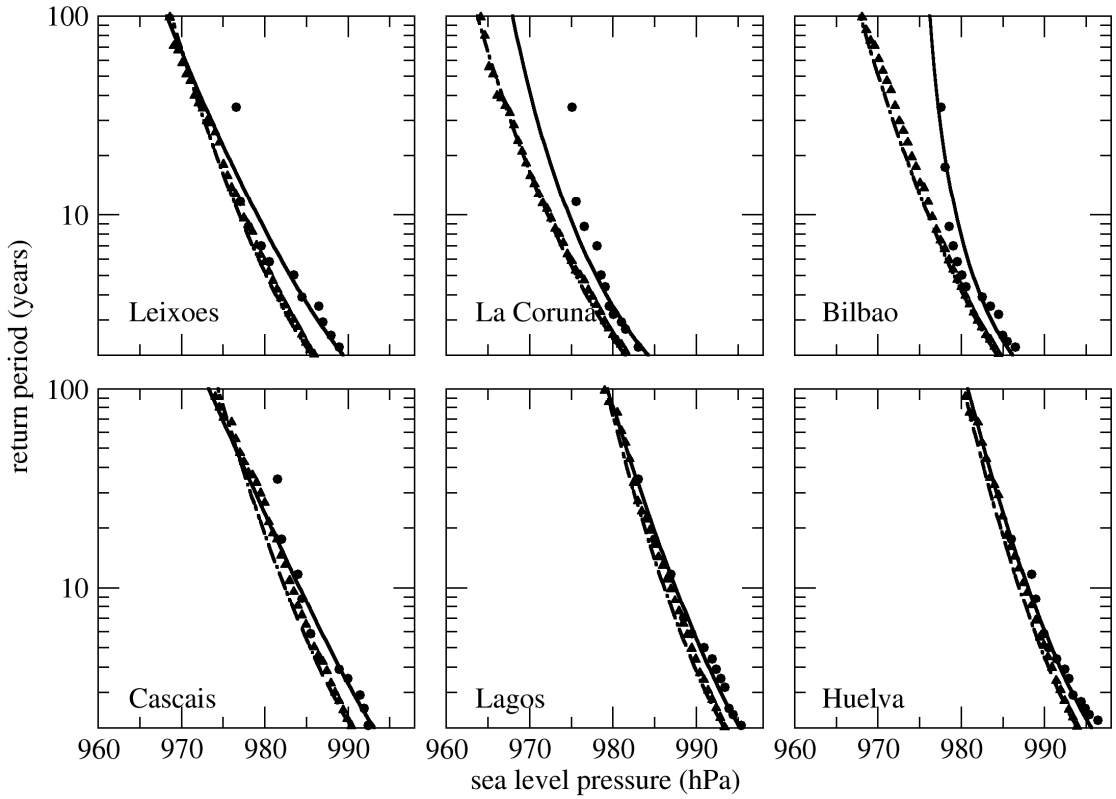


**Fig. 1 Validation of the atmospheric model: extreme low pressure at mean sea level between 1980 and 2014 at several stations (see Fig. 2 for locations) as given by ERA-Interim (circles and solid lines) and MiKlip (triangles and dashed lines). The symbols represent the empirical distribution function and the lines are adjusted GEV distributions**

### 2.3. Ocean modeling

Tides and surges are modeled separately. Tidal elevations are taken from the application (Fortunato et al. 2016) of the community model SELFE (Zhang and Baptista 2008) to a region in the NE Atlantic centered on the Iberian Peninsula (Fig. 2). SELFE is a semi-implicit finite element shallow water model, which targets cross-scale applications. The implicit nature of the model and the use of an Eulerian–Lagrangean method for advection avoid Courant number restrictions, allowing the use of large time steps. SELFE is

applied in depth-averaged barotropic mode. The grid has about 150,000 nodes and a resolution of about 250 m at the Portuguese coast, and 4000 m at the Spanish coast (Fig. 2). The time step is set to 5 minutes. The model application is forced at the ocean boundaries by tides from the global tide model FES2012 (Carrère et al. 2012) and by tidal potential. Eleven tidal constituents are imposed inside the domain through the tidal potential, and twenty-nine tidal constituents are forced at the boundary. Results for a 1-year simulation are harmonically analyzed, and tidal elevations for any specific period are obtained by harmonic synthesis.

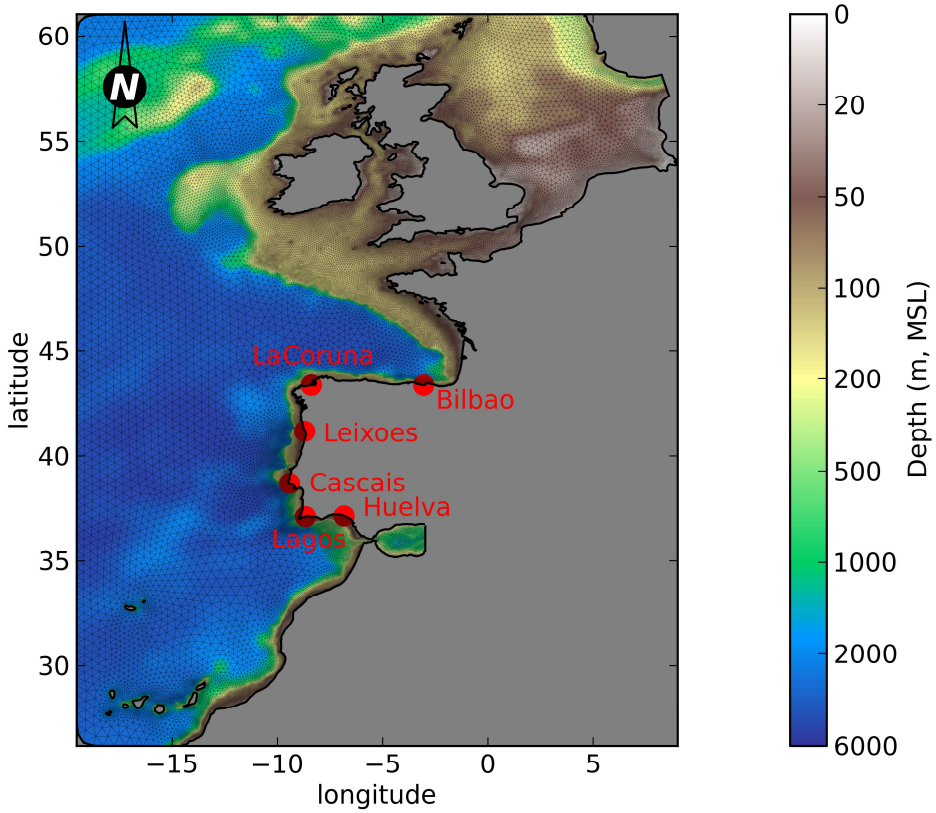


**Fig. 2 Ocean model domain, bathymetry, grid and tidal stations used in the analysis**

Water levels due to surges are simulated with SCHISM (Zhang et al. 2016). SCHISM evolved from the original SELFE model (v3.1dc), with many enhancements and upgrades for better accuracy and performance. The time step, the grid, the bathymetry and the model setup are the same as in the tidal simulations. Two types of surge simulations are performed. Present-day simulations are forced by winds and atmospheric pressure from the ERA-Interim reanalysis (Dee et al. 2011) for 1980-2016 (37 years). Near-future simulations are forced by MiKlip decadal predictions, dynamically downscaled with CCLM to 0.44° resolution over the EURO-CORDEX domain, for 2021-2024 (10x4 years).

Since the sensitivity of tides to modest SLR in this region is small, the mean sea level is considered invariant in all the simulations, and linearly added to the results when required. All simulations are run for one year. They start on the 22$^{nd}$ of December of the previous year so that a 10-day warm-up period can be discarded.

The total water level is obtained by adding the tidal and the surge signals. This approach implicitly neglects tide-surge interactions. These interactions are explained by non-linear terms in the shallow water equations and can be significant in shallow seas (e.g., Horsburgh and Wilson 2007) and inside estuaries (Fortunato et al. 2017). However, the tide-surge interactions are negligible in the study area (Fortunato et al. 2016) because the Iberian continental shelf is only a few tens-of-kilometers wide (Fig. 2).

The validation of the tidal model showed that its accuracy is very good in the southern part of the domain (i.e., up to the north of Spain) and declines further north. For instance, root-mean square errors for the five major tidal constituents vary between 1 and 10 cm (Fortunato et al. 2016). The tidal model is therefore considered validated.

The full tide-surge model is validated by comparing model results with observations from one tide gauge at each coast during the 2009-2010 Winter (Lagos, Cascais and La Coruna). This winter was very stormy in the region, in particular due to the passage of the Xynthia storm. This storm caused several floods in the Portuguese coast (Freire et al. 2016), and a major submersion on the French Aquitanian coast (Bertin et al. 2012). Results show that the model accurately reproduces both the low-frequency motions, dominated by the surge (Fig. 3), and the total sea surface elevations, dominated by the tidal signal (Fig. 4).

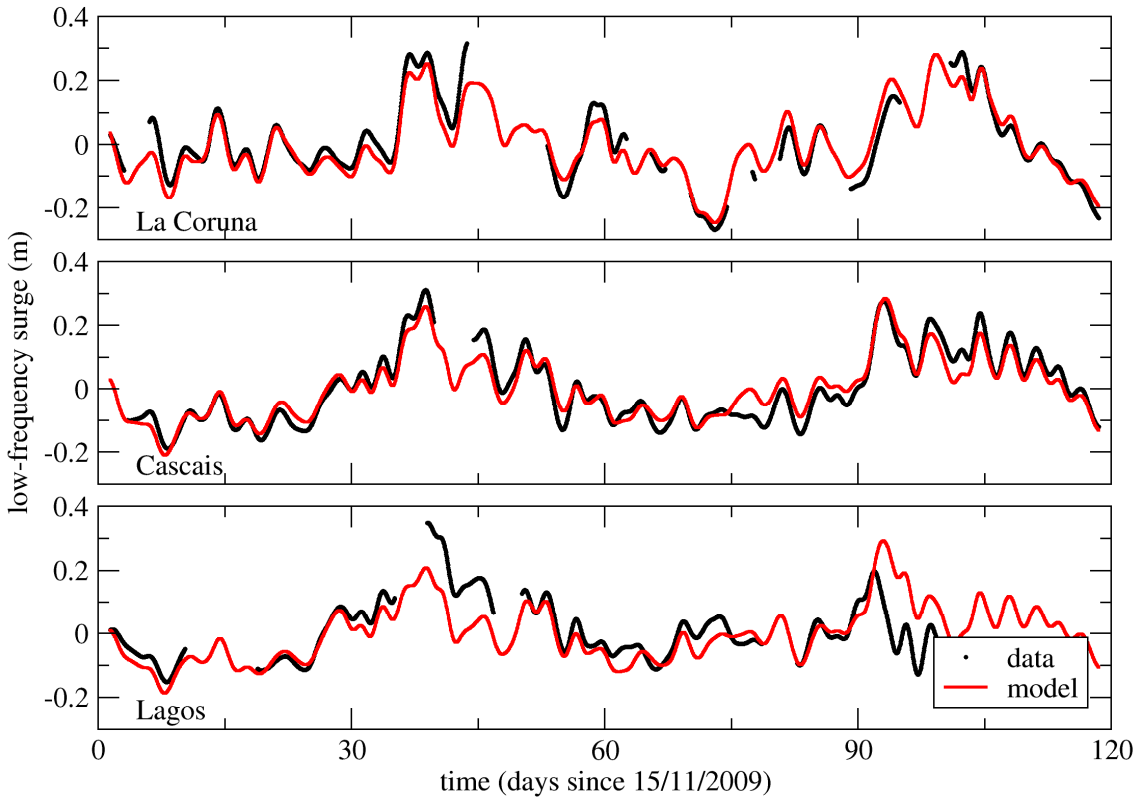


**Fig. 3 Validation of the ocean model at three stations for the winter 2009-2010: low-pass filtered observed and simulated elevations. Time series were obtained using a Demerliac filter, designed to remove the tidal signal**

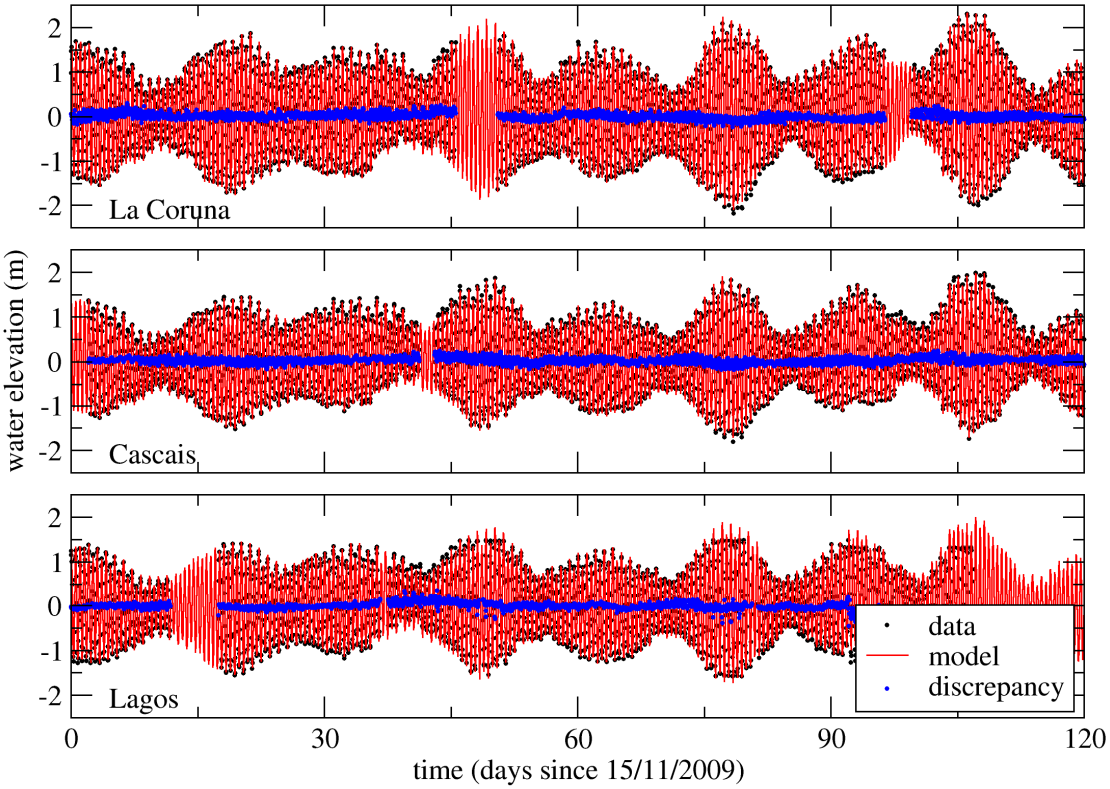


**Fig. 4 Validation of the ocean model at three stations for the winter 2009-2010: observed and simulated elevations, and differences between them. Unbiased root-mean square errors vary between 7 cm at La Coruna and Cascais, and 11 cm at Lagos**

## 2.4. Statistical analyses

Two distinct approaches were followed to determine extremes. The return periods of surges were determined with a traditional analysis of extreme values, while the total sea level was analyzed with a variation of the joint probability method proposed by Fortunato et al. (2013). Traditional analyses of extreme water levels work with limited numbers of extreme observations (typically a few tens of years). Statistical distribution functions must therefore be fit to the data to extrapolate the maximum levels for high return periods. In contrast, the approach proposed by Fortunato et al. (2013) leads to a number of annual maxima large enough to avoid the use of analytic functions.

To determine the return periods of surges for each period, Generalized Extreme Value (GEV) statistical distributions were fitted to the surge annual maxima assuming stationarity in location, scale and shape parameters. These parameters were determined using a maximum-likelihood estimator (Hosking, 1985). The return period T associated with a certain water level z is given by $T(z) = 1/(1-P(z))$, where P(z) is the probability of non-exceedance of z in one year. The mean water level at each station for the 1980-2016 storm surge simulations was removed from all the time series to provide a common vertical reference level: the present local mean sea level. This procedure was applied to sets of 37 and 40 years of data, for the present and the near-future, respectively. Extrapolating the extremes to return periods up to four times

the number of years used in the analysis is generally considered acceptable (Pugh and Woodworth, 2014). Here, the extrapolation is made to 100 years, well within the acceptable range. The 95% confidence limits were obtained by bootstrapping with replacement.

The use of ensembles to lengthen the data availability for extreme value analyses is a standard procedure and has been used previously by, e.g., van den Brink et al. (2005). Analyses (see Appendix) confirm that the atmospheric fields between the different members are not correlated, allowing them to be treated as independent realizations of the atmospheric circulation.

Sea surface elevations along the Iberian coast obtained with the model were statistically analyzed to determine extreme water levels for different return periods. The total sea level was examined with the method proposed by Fortunato et al. (2013), and then assessed by Fortunato et al. (2016). This method starts by generating a very large number of yearly time series of sea surface elevation by combining:

- the astronomical tide for a set of 19 consecutive years, which allows the consideration of the lunar cycle (ca. 18.6 years);
- the surge, with a variable phase lag with the tidal signal. These phase lags vary with one hour intervals between plus and minus 15 days, thereby ensuring that a given storm surge can occur at any time in the neap-spring tidal cycle. However, the seasonality of both tides and surges is also taken into account. For instance, a surge that occurs in January cannot be combined with a tide that occurs in March. The consideration of seasonality is important, as will be shown below.

This procedure provides a very large number of hypothetical annual series for each mean sea level scenario. Here, 506,160 (i.e. 24x19x30x37) yearly time series were generated for the present (1980-2016), and 547,200 (i.e. 24x19x30x40) for the near-future (2021-2024). The set of all maxima in all series makes it possible to determine the probability of occurrence of a certain extreme level. An analysis of this method showed that 100-year return period extremes can be determined from 30-40 years of data with errors of a few centimeters (Fortunato et al., 2016).

## 3. Results and discussion

### 3.1. Storm surges

Model results were first analyzed at two representative tidal stations along each of the northern (La Coruna and Bilbao), western (Leixões and Cascais) and southern (Lagos and Huelva) coasts of the Iberian Peninsula (Fig. 2). Extreme values exhibit a significant spatial variability (Fig. 5). The differences in the 100-year return period surge, based on the GEV distributions, vary between -9 cm at Leixões and +12 cm (Huelva and La Coruna).

In general, the west coast stations exhibit the smallest changes. The GEV distributions indicate that their maximum surge increases slightly for the low return periods (below 10 years) and decreases for the higher return periods (above 40 years). However, this distinct behavior between the high and the low return periods is not clear in the empirical distributions. It is thus possible that the reduction of extreme surges for high return periods along the west coast stems from errors in the adjustment of the GEV functions. Lagos, which is located on the south coast but very close to the west coast, shows a similar behavior, with very small changes in the maximum surge. Overall, these changes are considered negligible.

At the northern and southern stations, the maximum surge increases for all the return periods up to 100 years. The growth of the surges in the north coast stations may be over-predicted. Indeed, the validation of

the atmospheric model showed that the low pressure extremes were under-predicted relative to the ERA-Interim reanalyses (Fig. 1). So, overall, extreme surges are expected to change very little, except at the southernmost areas.

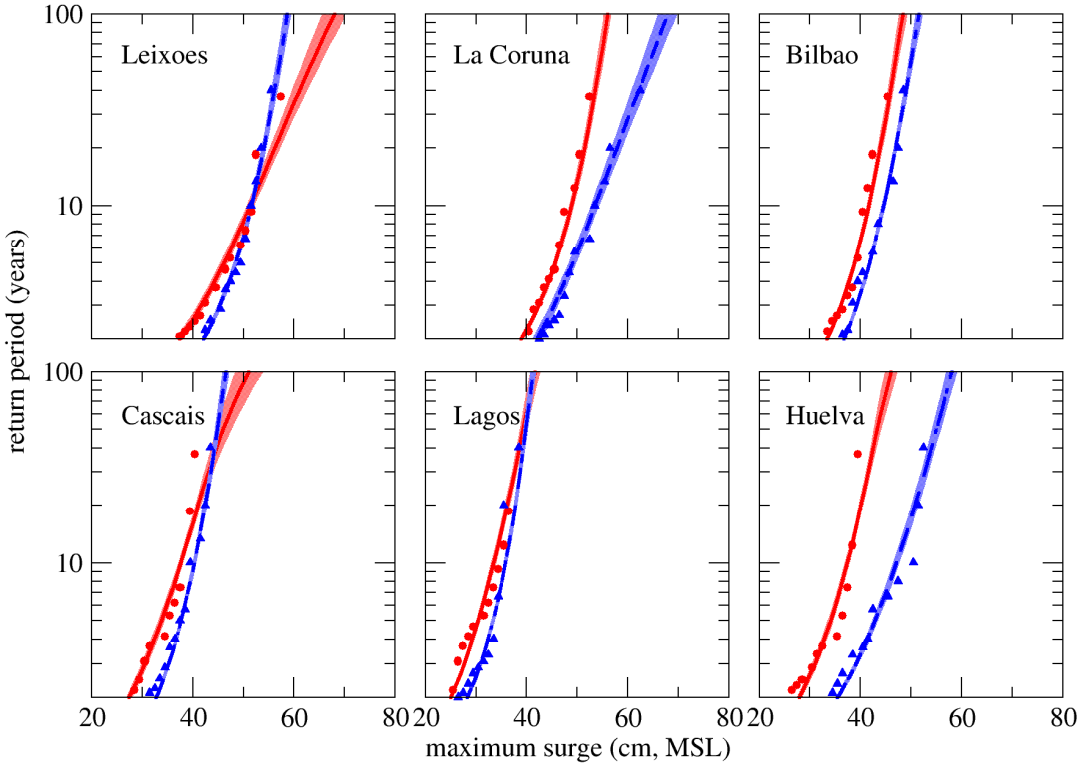


**Fig. 5 Changes in extreme storm surges at selected stations between the present (1980-2016, circles and solid lines) and the future (2021-2024, triangles and dashed lines). The symbols represent the empirical distribution law, and the lines are adjusted GEV functions. The shaded areas represent the 95% confidence limits, obtained by bootstrapping with replacement**

In order to search for seasonal behaviors, means and standard deviations were computed for each hour of the year for the two databases (present and future), and the resulting time series of the mean and of the mean plus the standard deviation were then further averaged for each month (Fig. 6). Results reveal marked seasonal patterns. Using the mean plus the standard deviation as a proxy for the storminess, results show that early spring (April) and the fall are presently the most severe periods of the year at all stations. Conversely, the minimum storminess occurs in the summer months. The decadal predictions indicate a significant increase of the surges in the winter months, in particular at the northern stations. The increase in storminess in January is observed both in the mean and in the standard deviation of the surge. Simultaneously, storminess decreases in April at the southern stations. Due to this behavior, the most severe month in terms of surges will shift from April to January at the stations in the north and west coasts (Fig. 6).

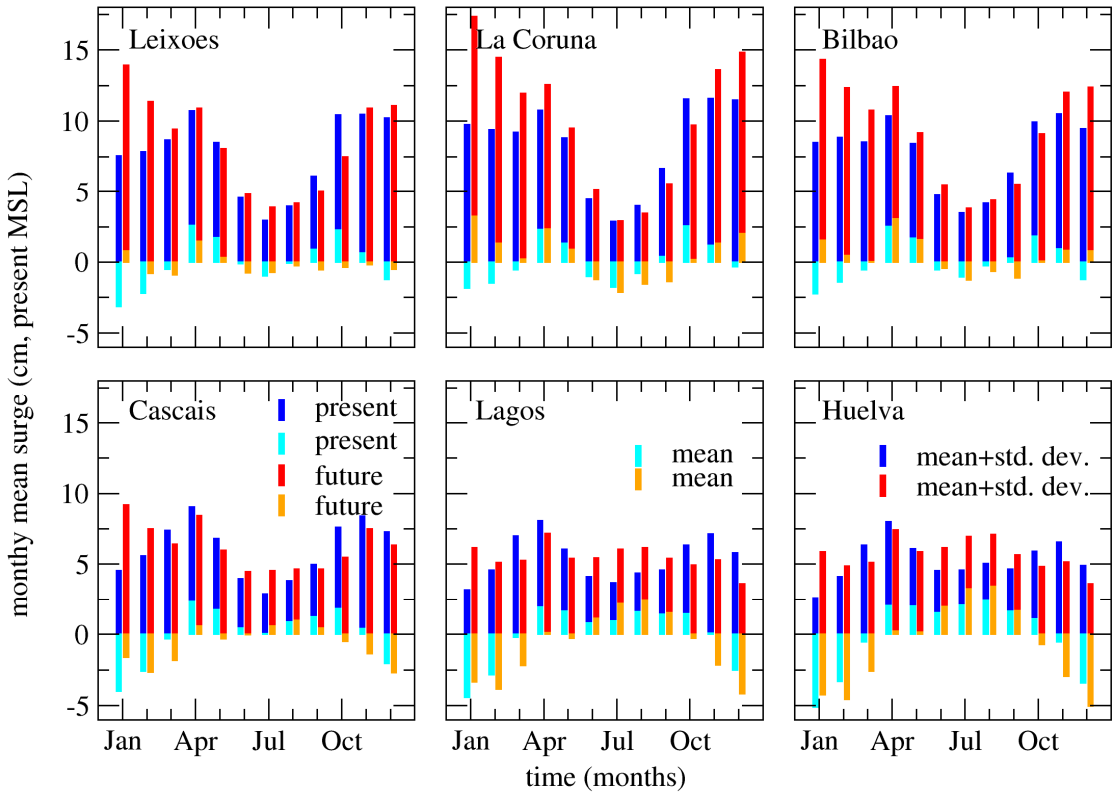


**Fig. 6 Monthly variation of storm surges at selected stations: monthly averages (lower bars) and average plus standard deviations (upper bars) for present (left bars) and future (right bars) conditions**

### 3.2. Extreme water levels

Water levels during 1980-2016 and 2021-2024 were determined by adding tides, storm surges and the mean sea level. The analysis focuses on the changes between the two periods, so the statistics of each of these intervals were considered stationary. To be consistent with this hypothesis, the variability of the mean sea level within each of these intervals was neglected. The mean sea level in 2021-2024 was assumed to be 11 cm higher than in 1980-2016, as explained in the previous section.

The extreme sea levels and their evolution are discussed by examining the spatial variation of the water levels for a 100 year return period (Fig. 7). Extreme sea levels show a latitudinal gradient, growing northward. As shown by Fortunato et al. (2016), this behavior is mostly due to the growth of the tidal amplitudes from the south to the north. However, storm surges also play a small role, since they are smallest in the southern coast and increase northward along the west coast (Fig. 6). While the spatial evolution of the extreme water levels is generally smooth, there are localized growths at the head of the rias, in the northwest of Spain. These growths are due to the funnel shape of these water bodies, which locally amplifies the tidal amplitudes.

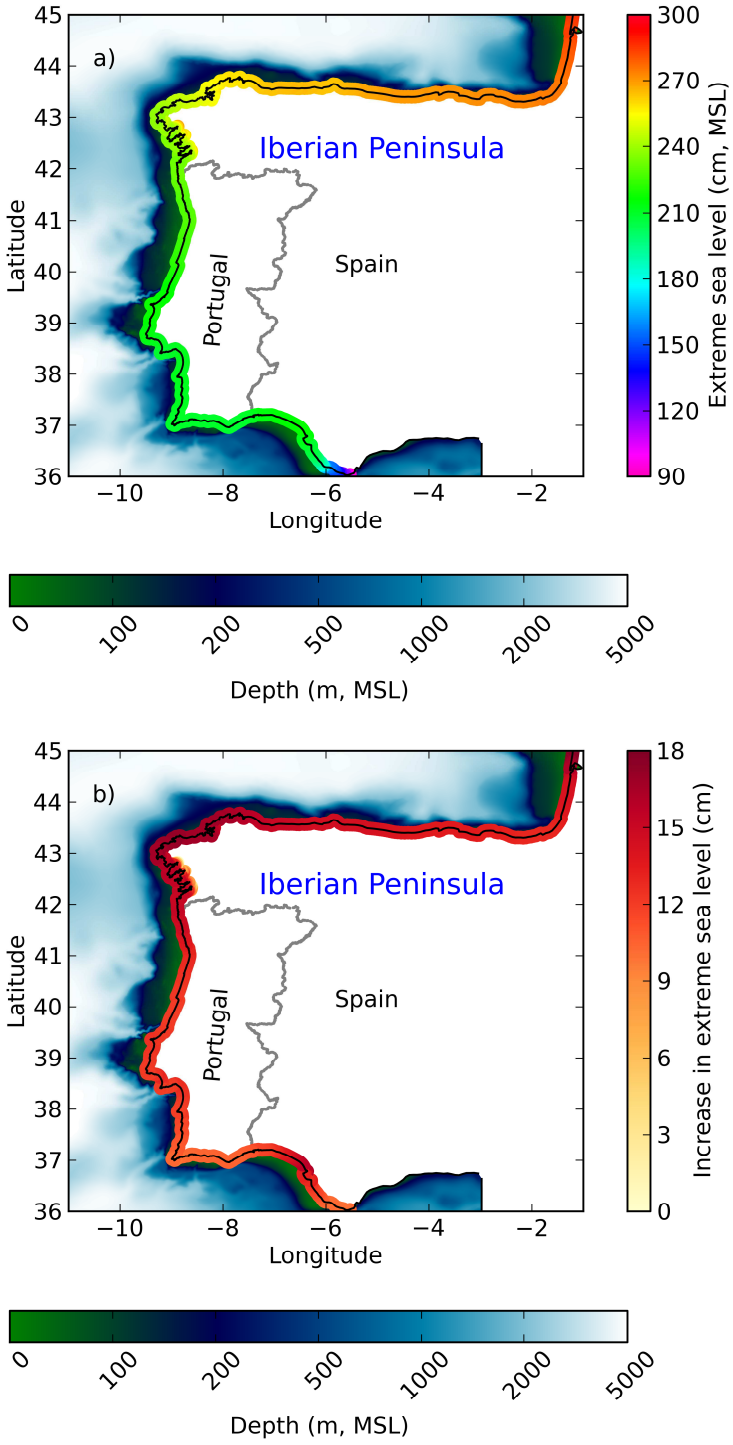


**Fig. 7 Evolution of extreme sea levels along the Iberian Atlantic coast for a return period of 100 years: a) present (1980-2016); b) increase from present to future (2021-2024)**

Extreme sea levels, represented by 100 year return periods, are predicted to grow by 10-13 cm along most of the Iberian Atlantic coast (Fig. 7b). This growth will increase only slightly from about 10 cm near the Strait of Gibraltar to 13 cm near the French border. The exceptions are the heads of the Galician rias (north of Spain) where the growth is smaller (typically 0-10 cm). The growth of the extreme sea levels is thus mostly due to the mean SLR.

These conclusions on the evolution of the extreme sea levels (100 year return period) may appear to contradict the growth of storminess in early winter. Indeed, this growth suggests that the extreme sea levels would grow beyond the SLR. This expected behavior is not verified in the present analysis. A possible explanation for this apparent discrepancy lies in the seasonal effects identified above. Given the importance of the tidal range compared to the surges, the highest sea levels will tend to occur during equinoxial tides, i.e., in early March and mid-September (Fig. 8). Because surges are higher in March than in September (Fig. 6), March is the critical month in terms of extreme sea levels. The seasonal analysis of the surges indicates that, in March, surges actually decrease in the southern part of the domain (Huelva, Lagos and Cascais), and increase in the north (Leixões, La Coruna and Bilbao). This result is consistent with the slight northward growth of the extreme sea levels. Hence, it appears that the overall growth of storm surges, which occurs primarily in January, will have little effect on the extreme sea levels.

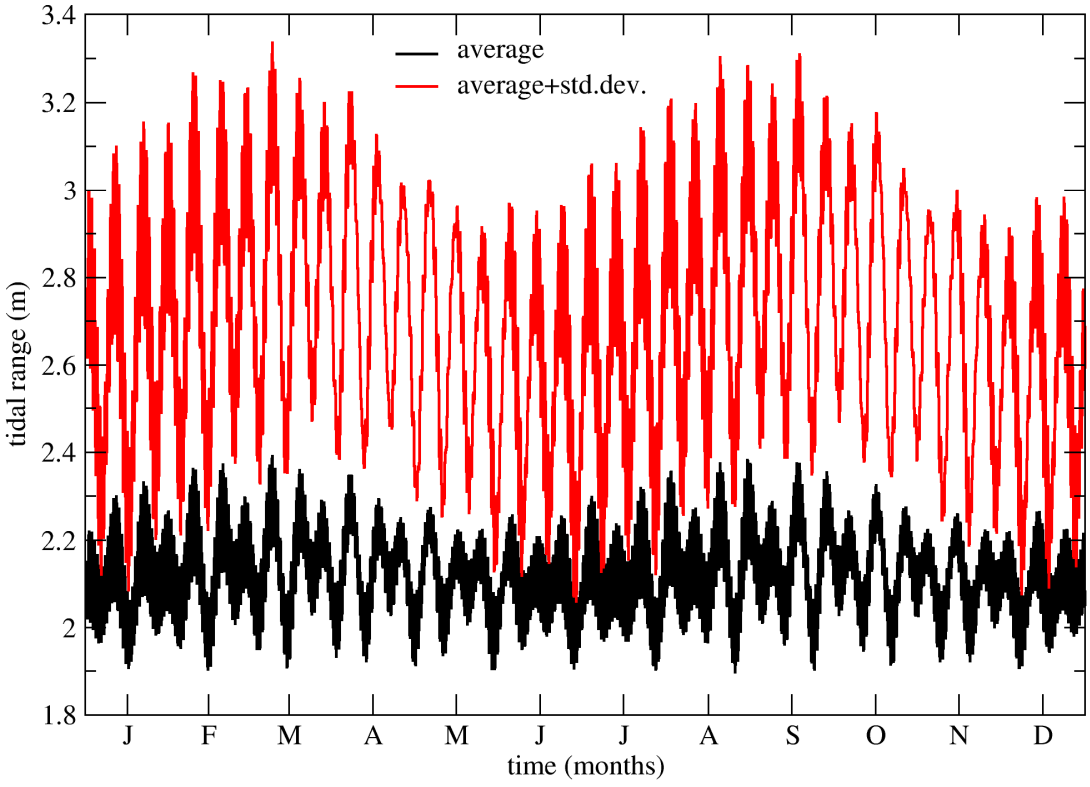


**Fig. 8 Seasonality of the tides at Cascais, highlighting the occurrence of equinoxial tides in early March and mid-September. The means and standard deviations were computed from a sample of 19 consecutive years (1991-2009)**

## 4. Summary and conclusions

Multi-decadal databases of storm surges and total sea levels were generated for the Atlantic Iberian shelf. Each database has about 40 years of simulations for the "present" (1980-2016) and the near-future (2021-2024, with 10 realizations per year). The "present" and "future" thus represent 1998 and 2022, respectively. Storm surges were simulated with a shallow water model (SCHISM), in depth-averaged barotropic mode. Simulations were forced by the ERA-Interim reanalyses (present) and the MiKlip decadal predictions from the MPI-ESM-LR model (near-future); validation of pressure extremes in the MPI-ESM-LR model showed only a slight bias from reanalyses. Tides were taken from Fortunato et al. (2016) and added linearly to the surges, since tide-surge interactions are negligible in the study region. The long duration of the datasets allowed the performance of statistical analyses and the examination of the short-term impact of changes in the climate system, due to both natural internal variability and forced climate change, on storm surges and water levels in the Iberian Atlantic coast.

In general, the surges will increase by a few centimeters between 1998 and 2022. For return periods around one hundred years, this growth can reach about 10 cm in the south coast. In the west coast, this growth is smaller and there can even be a reduction for the higher return periods. Finally, the model shows increases of the order of 10 cm in the north coast, but this behavior may be due to a bias in the atmospheric model.

The analysis of the total sea levels, including the effect of tides, surges and mean sea level, shows that the changes in extreme sea levels (100 year return period) will be mostly due to the mean SLR. The apparent discrepancy between the behaviors of extreme storm surges and sea levels is explained by the seasonal variability of the tides and surges: surges will increase mostly in early winter, while tides are largest in late winter. Hence, the extremes tend to occur in late winter, and will be unaffected by the growth of surges in the early winter.

While the increase in storminess in early winter may not have a significant effect on coastal flooding, other adverse effects are likely to occur. In particular, coastal erosion is bound to be aggravated by the higher winter storminess. Further studies are required to examine this effect in detail and, in particular, waves will need to be considered in the simulations.

The ability of the decadal projections to determine if a particular region will be prone to storms, floods or draughts in a given period can be exploited by the civil protection and water authorities to improve planning and management, and ultimately save lives, reduce costs or optimize agricultural production. Yet, because decadal predictions are still in their infancy, their potential remains to be fully exploited. This paper constitutes a first attempt to exploit decadal predictions to determine the future storminess at regional scales.

## Appendix

The statistical analyses presented in the paper used several predictions for each year. The predictions vary in the way the atmospheric model was initialized (10 different ensemble members) and, in some cases, the lead year (i.e., the number of years since the beginning of the simulation). The question arises as to what extent different daily predictions for the same year exhibit any type of similarity or correlation. The answer to this question is important to establish whether or not the time series represent independent realizations of the atmospheric state.

It was hypothesized that the different predictions for the same year were uncorrelated, except for the seasonal signal. This hypothesis was verified for the mean sea level pressure at Cascais, using the predictions for 1980-2011. For each year, we used 40 predictions, corresponding to 10 ensemble members and 4 lead years (lead years 7 through10).

The verification proceeded as follows. First, daily and monthly averages of mean sea level pressures at Cascais were computed for the 1280 time series (10 ensemble members, 32 years and 4 lead years). Then, the climatology (means of the monthly means) was determined and subtracted from the daily time series to obtain the daily residuals. Finally, the correlation for each pair of daily residuals series for the same year was determined. Results show that there is no correlation between predictions (Fig. 9), thereby validating their use as independent time series.

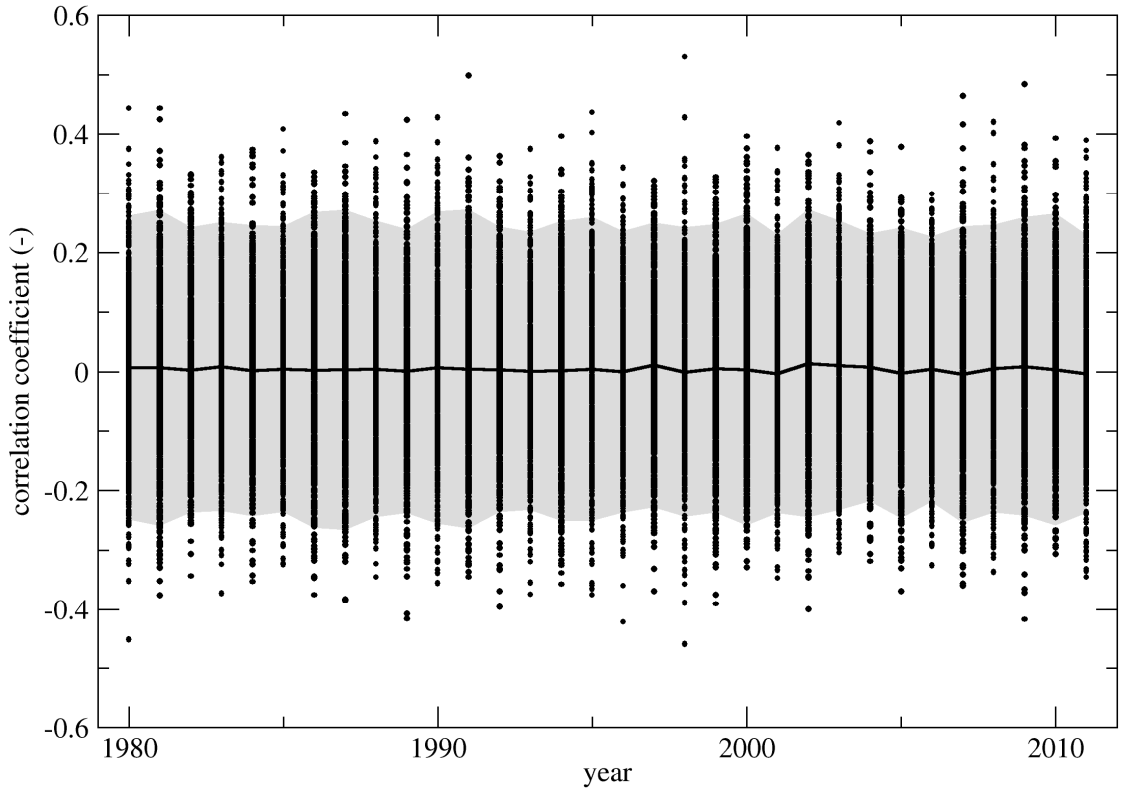


**Fig. 9 Correlation analysis between predictions for the same year. Each circle represents the correlation coefficient between two time-series of predicted residuals for the same year at Cascais. The solid line shows their mean, and the shaded area shows the 95% confidence interval.**

**Acknowledgements**

This work was partially funded by the European Commission through the H2020 project BINGO (Grant Agreement Number 641739). MR was also partially funded by a post-doctoral grant from FCT – Fundação para a Ciência e a Tecnologia (SFRH/BPD/87512/2012). This work made use of results produced with the support of the Portuguese National Grid Initiative; more information in

https://wiki.ncg.ingrid.pt. The climate simulations were performed at the German Climate Computing Centre (DKRZ). We thank Prof. Joseph Zhang for the model SCHISM, Dr. Alberto Azevedo for help in processing data, Drs. Elsa Alves and Manuel Oliveira for useful discussions, and two anonymous reviewers for constructive criticism.

**References**

Andrade C, Pires O, Taborda R, Freitas MC (2007) Projecting future changes in wave climate and coastal response in Portugal by the end of the 21st century. *Journal of Coastal Research*, **Special Issue 50**, 263-267.

Antunes C (2016) Subida do Nível Médio do Mar em Cascais, revisão da taxa actual. Actas das 4.as Jornadas de Engenharia Hidrográfica, Instituto Hidrográfico (in Portuguese). ISBN - 978-989-705-097-8.

Bertin X, Bruneau N, Breilh J-F, Fortunato AB, Karpytchev M (2012). Importance of wave age and resonance in storm surges: The case Xynthia, Bay of Biscay. *Ocean Modelling*, **42**, 1: 16-30. DOI: 10.1016/j.ocemod.2011.11.001

Bordbar MH, Martin T, Latif M, Park W (2017) Role of internal variability in recent decadal to multidecadal tropical Pacific climate changes. *Geophysical Research Letters*, **44**, 4246-4255. DOI: 10.1002/2016GL072355.

Camus P, Losada IJ, Izaguirre C, Espejo A, Menéndez M, Pérez J (2017) Statistical wave climate projections for coastal impact assessments. *Earth's Future*, **5**/9, 918-933. DOI: 10.1002/2017EF000609

Carrère L, Lyard F, Cancet M, Guillot A, Roblou L (2012) FES2012: A new global tidal model taking advantage of nearly 20 years of altimetry, *Proceedings of meeting 20 Years of Altimetry*.

Charles E, Idier D, Delecluse P, Déqué M, Le Cozannet G (2012) Climate change impact on waves in the Bay of Biscay, France. *Ocean Dynamics*, **62**/6, 831-848. DOI: 10.1007/s1023601205348.

Chaumillon E, Bertin X, Fortunato AB, Bajo M, Schneider J-L, Dezileau L, Walsh JP, Michelot A, Chauveau E, Créach A, Hénaff A, Sauzeau T, Waeles B, Gervais B, Jan G, Baumann J, Breilh J-F, Pedreros R (2017) Storm-induced marine flooding: Lessons from a multidisciplinary approach. *Earth-Science Reviews*, **165**, 151-184. DOI: 10.1016/j.earscirev.2016.12.005

Dangendorf S, Marcos M, Wöppelmann G, Conrad CP, Frederikse T, Riva R (2017) Reassessment of 20th century global mean sea level rise. *Proceedings of the National Academy of Sciences*, **114**(23), 5946-5951. DOI: 10.1073/pnas.1616007114

Dee DP, Uppala SM, Simmons AJ, Berrisford P, Poli P, Kobayashi S, Andrae U, Balmaseda MA, Balsamo G, Bauer P, Bechtold P, Beljaars ACM, van de Berg L, Bidlot J, Bormann N, Delsol C, Dragani R, Fuentes M, Geer AJ, Haimberger L, Healy SB, Hersbach H, Hólm EV, Isaksen L, Kållberg P, Köhler M, Matricardi M, McNally AP, Monge-Sanz BM, Morcrette J-J, Park B-K, Peubey C, de Rosnay P, Tavolato C, Thépaut J-N, Vitart F (2011) The ERA-Interim reanalysis: configuration and performance of the data assimilation system. *Quarterly Journal of the Royal Meteorological Society*, **137**, 553–597. DOI: 10.1002/qj.828.

Fortunato AB, Rodrigues M, Dias JM, Lopes C, Oliveira A (2013) Generating inundation maps for a coastal lagoon: A case study in the Ria de Aveiro (Portugal). *Ocean Engineering*, **64**(1), 60-71. DOI: 10.1016/j.oceaneng.2013.02.020

Fortunato AB, Li K, Bertin X, Rodrigues M, Miguez BM (2016) Determination of extreme sea levels along the Iberian Atlantic coast. *Ocean Engineering*, **111**(1), 471-482. DOI: 10.1016/j.oceaneng.2015.11.031

Fortunato AB, Freire P, Bertin X, Rodrigues M, Ferreira J, Liberato ML (2017) A numerical study of the February 15, 1941 storm in the Tagus estuary. *Continental Shelf Research*, **144**, 50-64. doi: 10.1016/j.csr.2017.06.023

Freire P, Tavares AO, Sá L, Oliveira A, Fortunato AB, Santos PP, Rilo A, Gomes JL, Rogeiro J, Pablo R, Pinto PJ (2016) A local-scale approach to estuarine flood risk management, *Natural Hazards*, **84**(3), 1705-1739. DOI: 10.1007/s11069-016-2510-y

Freitas JG, Dias JA (2013) 1941 windstorm effects on the Portuguese Coast. What lessons for the future? *Journal of Coastal Research*, **Special Issue 65**, 714-719.

Garnier E, Ciavola P, Spencer T, Ferreira Ó, Armaroli C, McIvor A (2018). Historical analysis of storm events: Case studies in France, England, Portugal and Italy. *Coastal Engineering*, **134**, 10-23. DOI: 10.1016/j.coastaleng.2017.06.014.

Giorgetta MA, Jungclaus J, Reick CH, Legutke S, Bader J, Böttinger M, Brovkin V, Crueger T, Esch M, Fieg K, Glushak K, Gayler V, Haak H, Hollweg H-D, Ilyina T, Kinne S, Kornblueh L, Matei D, Mauritsen T, Mikolajewicz U, Mueller W, Notz D, Pithan F, Raddatz T, Rast S, Redler R, Roeckner E, Schmidt H, Schnur R, Segschneider J, Six KD, Stockhause M, Timmreck C, Wegner J, Widmann H, Wieners KH, Claussen M, Marotzke J, Stevens B (2013) Climate and carbon cycle changes from 1850 to 2100 in MPI-ESM simulations for the Coupled Model Intercomparison Project phase 5. *Journal of Advances in Modeling Earth Systems*, **5**, 572-597. DOI:10.1002/jame.20038.

Guérin T, Bertin X, Coulombier T, de Bakker A (2018) Impacts of wave-induced circulation in the surf zone on wave setup. *Ocean Modelling*, **123**, 86-97. DOI: 10.1016/j.ocemod.2018.01.006.

Guerreiro M, Fortunato AB, Freire P, Rilo A, Taborda R, Freitas MC, Andrade C, Silva T, Rodrigues M, Bertin X, Azevedo A (2015) Evolution of the hydrodynamics of the Tagus estuary (Portugal) in the 21st century. *Journal of Integrated Coastal Zone Management*, **15**(1): 65-80. DOI: 10.5894/rgci515

Horsburgh KJ, Wilson C (2007) Tide-surge interaction and its role in the distribution of surge residuals in the North Sea. *Journal of Geophysical Research*. **112(**C08003), DOI: 10.1029/2006JC004033

Hosking JRM (1985) Algorithm AS2015 : Maximum-likelihood estimation of the parameters of the Generalized Extreme-Value distribution. *Journal of the Royal Statistical Society. Series C (Applied Statistics)*,**34(**3): 301-310.

Idier D, Paris F, Le Cozannet G, Boulahya F, Dumas F (2017) Sea-level rise impacts on the tides of the European Shelf. *Continental Shelf Research*, **137**: 56-71. DOI: 10.1016/j.csr.2017.01.007.

Jacob D, Petersen J, Eggert B, Alias A, Christensen OB, Bouwer LM, Braun A, Colette A, Déqué M, Georgievski G, Georgopoulou E, Gobiet A, Menut L, Nikulin G, Haensler A, Hempelmann N, Jones C, Keuler K, Kovats S, Kröner N, Kotlarski S, Kriegsmann A, Martin E, van Meijgaard E, Moseley C, Pfeifer S, Preuschmann S, Radermacher C, Radtke K, Rechid D, Rounsevell M, Samuelsson P, Somot S, Soussana J-F, Teichmann C, Valentini R, Vautard R, Weber B, Yiou P (2014) EURO-CORDEX: new high-resolution climate change projections for European impact research. *Regional Environmental Change*, **14**, 563–578. DOI: 10.1007/s10113-013-0499-2.

Kadow C, Illing S, Kunst O, Rust HW, Pohlmann H, Müller WA, Cubasch U (2016) Evaluation of forecasts by accuracy and spread in the MiKlip decadal climate prediction system. *Meteorologische Zeitschrift*, **25**(6), 631 – 643.

Kruschke T, Rust HW, Kadow C, Leckebusch GC, Ulbrich U (2014) Evaluating decadal predictions of northern hemispheric cyclone frequencies. *Tellus A: Dynamic Meteorology and Oceanography*, **66**, 1-15, 22830, DOI: 10.3402/tellusa.v66.22830

Kruschke T, Rust HW, Kadow C, Muller WA, Pohlmann H, Leckebusch GC, Ulbrich U (2016) Probabilistic evaluation of decadal prediction skill regarding Northern hemisphere winter storms. *Meteorologishe Zeitschrift*, **25(**6), 721-738.

Marcos M, Woodworth PL (2017) Spatiotemporal changes in extreme sea levels along the coasts of the North Atlantic and the Gulf of Mexico. *Journal of Geophysical Research: Oceans*, **122**. DOI: 10.1002/2017JC013065

Marotzke J, Müller WA, Vamborg FS, Becker P, Cubasch U, Feldmann H, Kaspar F, Kottmeier C, Marini C, Polkova I, Prömmel K, Rust HW, Stammer D, Ulbrich U, Kadow C, Köhl A, Kröger J, Kruschke T, Pinto JG, Pohlmann H, Reyers M, Schröder M, Sienz F, Timmreck C, Ziese M (2016) MiKlip: a national research project on decadal climate prediction. *Bull. Amer. Meteor. Soc.*, **97**, 2379-2394. DOI: 10.1175/BAMS-D-15-00184.1

Muir-Wood R (2011) The 1941 February 15th Windstorm in the Iberian Peninsula. Mapfre. http://www.mapfre.com/mapfrere/docs/html/revistas/trebol/n56/docs/Articulo1en.pdf.

Mueller WA, Baehr J, Haak H, Jungclaus JH, Kröger J, Matei D, Notz D, Pohlmann H, Storch JS, Marotzke J (2012) Forecast skill of multi-year seasonal means in the decadal prediction system of the Max Planck Institute for Meteorology. *Geophysical Research Letters*, **39**(22). DOI: 10.1029/2012GL053326

Nauels A, Meinshausen M, Mengel M, Lorbacher K, Wigley TML (2017) Synthesizing long-term sea level rise projections – the MAGICC sea level model v2.0. *Geoscientific Model Development*, **10**, 2495-2524. DOI: 10.5194/gmd-10-2495-2017

Perez J, Menendez M, Camus P, Mendez FJ, Losada IJ (2015). Statistical multi-model climate projections of surface ocean waves in Europe. *Ocean Modelling*, **96**, 161-170. DOI: 10.1016/j.ocemod.2015.06.001

Pickering MD, Horsburgh KJ, Blundell JR, Hirschi JJ-M, Nicholls RJ, Verlaan M, Wells NC (2017) The impact of future sea-level rise on the global tides. *Continental Shelf Research*, **142**, 50-68. DOI: 101016/j.csr.2017.02.004.

Pohlmann H, Mueller WA, Kulkarni K, Kameswarrao M, Matei D, Vamborg FSE, Kadow C, Illing S, Marotzke J (2013) Improved forecast skill in the tropics in the new MiKlip decadal climate predictions. *Geophysical Research Letters*, **40**(21), 5798-5802. DOI: 10.1002/2013GL058051

Pugh D, Woodworth PL (2014) *Sea-level Science: understanding tides, surges, tsunamis and mean sea-level changes* 407, Cambridge University Press.

Rockel B, Will A, Hense A (2008) The regional climate model COSMO-CLM (CCLM), *Meteorologische Zeitschrift*, **17**(4), 347-348. DOI: 10.1127/0941-2948/2008/0309

Santamaría-Gómez A, Gravelle M, Dangendorf S, Marcos M, Spada G, Wöppelmann G (2017) Uncertainty of the 20th century sea-level rise due to vertical land motion errors. *Earth and Planetary Science Letters*, **473**, 24-32, DOI: 10.1016/j.epsl.2017.05.038.

Smith DM, Cusack S, Colman AW, Folland CK, Harris GR, Murphy JM (2007) Improved surface temperature prediction for the coming decade from a global climate model. *Science*, **317**(5839): 796-799. DOI: 10.1126/science.1139540

Thompson PR, Mitchum GT, Vonesch C, Li J (2013). Variability of winter storminess in the eastern United States during the twentieth century from tide gauges. *Journal of Climate*, **26**, 9713–9726, DOI:10.1175/JCLI-D-12-00561.1

Tiedtke M (1989) A comprehensive mass flux scheme for cumulus parameterization in large-scale models. *Monthly Weather Review*, **117**, 1779–1799. DOI: 10.1175/1520-0493(1989)117<1779:ACMFSF>2.0.CO;2

van den Brink HW, Konnen GP, Opsteegh JD, van Oldenborgh GJ, Burgers G (2005). Estimating return periods of extreme events from ECMWF seasonal forecast ensembles. *International Journal of Climatology*, **25**: 1345 – 1354

Van Vuuren DP, Edmonds J, Kainuma M, Riahi K, Thomson A, Hibbard K, Hurtt GC, Kram T, Krey V, Lamarque J-F, Masui T, Meinshausen M, Nakicenovic N, Smith SJ, Rose SK (2011) The

representative concentration pathways: an overview. *Climatic Change*, **109**, 5. DOI: 10.1007/s10584-011-0148-z

Vousdoukas MI, Voukouvalas E, Annunziato A, Giardino A, Feyen L (2016) Projections of extreme storm surge levels along Europe, *Climate Dynamics*, **47**(9-10), 3171-3190. DOI: 10.1007/s00382-016-3019-5

Vousdoukas MI, Mentaschi L, Voukouvalas E, Verlaan M, Feyen L (2017). Extreme sea levels on the rise along Europe's coasts. *Earths Future*, **5**(3), 304-323. DOI: 10.1002/2016EF000505

Wahl T, Haigh ID, Nicholls RJ, Arns A, Dangendorf S, Hinkel J, Slangen ABA (2017) Understanding extreme sea levels for broad-scale coastal impact and adaptation analysis. *Nature Communications*, **8**, Article Number: 16075. DOI: 10.1038/ncomms16075

Zhang Y, Baptista AM (2008) SELFE: a semi-implicit Eulerian-Lagrangian finite element model for cross-scale ocean circulation. *Ocean Modelling*, **21**(3–4), 71–96. DOI: 10.1016/j.ocemod.2007.11.005.

Zhang YJ, Ye F, Stanev EV, Grashorn S (2016) Seamless cross-scale modeling with SCHISM. *Ocean Modeling*, **102**, 64–81. DOI: 10.1016/J.OCEMOD.2016.05.002.